Technical report: Gaussian approximation for superpositional sensors

Nannuru Santosh and Mark Coates

This report discusses approximations related to the random finite set based filters for superpositional sensors [1], [2]. To derive computationally tractable approximate filters of PHD, CPHD, multi-Bernoulli and hybrid multi-Bernoulli CPHD, a key step involves approximating the density of the predicted observation vector with a Gaussian distribution. This approximation allows us to analytically simplify an integral and provide compuational tractability. In this technical report we analyze the error introduced in the integral because of the Gaussian approximation.

I. Validation of the integral under Gaussian assumption

Let Ξ be a random finite set with multitarget density function $f_{\Xi}(W)$. Let the PHD and second factorial moment of the random finite set Ξ be denoted by $D(\mathbf{x})$ and $D(\{\mathbf{x}_1, \mathbf{x}_2\})$. The random vector $\mathbf{y}$ is a function of the random finite set Ξ and has the following superpositional form

$$\mathbf{y} = \zeta(\Xi) = \sum_{\mathbf{x} \epsilon \Xi} g(\mathbf{x}). \tag{1}$$

From Section V of the draft, to derive computationally tractable filter update equations, we have to evaluate the following set integral

$$\mathbf{I} = \int \mathcal{N}_{\Sigma_0}(\mathbf{y}_0 - \zeta(W))\, f_{\Xi}(W) \delta W. \tag{2}$$

By applying the change of variables formula for set integrals [3], we can express the above set integral in the following standard integral form

$$\mathbf{I} = \int \mathcal{N}_{\Sigma_0}(\mathbf{y}_0 - \mathbf{y})\, Q(\mathbf{y}) d\mathbf{y} \tag{3}$$

where $Q(\mathbf{y})$ is the probability density function of the random vector $\mathbf{y}$. Even though in the above form the integral is simpler to evaluate than the set integral, without making any assumptions on the density function $Q(\mathbf{y})$ the integral is analytically intractable. To make the above integral tractable, in the paper we use the approximation that the density function $Q(\mathbf{y})$ is a Gaussian density function. The mean vector and the covariance matrix of this Gaussian density function can be found using the Campbell's theorem. If $\boldsymbol{\mu}_Q$ and Σ_Q are the mean and covariance matrix then we have the approximation $Q(\mathbf{y}) \approx \mathcal{N}_{\Sigma_Q}(\boldsymbol{\mu}_Q - \mathbf{y})$.

From Campbell's theorem we have

$$\boldsymbol{\mu}_Q = E[(\mathbf{y})] = \int g(\mathbf{x})\, D(\mathbf{x}) d\mathbf{x} \tag{4}$$

$$\Sigma_Q = E[(\mathbf{y}-\boldsymbol{\mu})(\mathbf{y}-\boldsymbol{\mu})^T] \tag{5}$$

$$= \int g(\mathbf{x})\, g(\mathbf{x})^T\, D(\mathbf{x}) d\mathbf{x} + \int\int g(\mathbf{x}_1)\, g(\mathbf{x}_2)^T\, \tilde{D}(\{\mathbf{x}_1, \mathbf{x}_2\}) d\mathbf{x}_1 d\mathbf{x}_2 \tag{6}$$

$$\text{where } \tilde{D}(\{\mathbf{x}_1, \mathbf{x}_2\}) = D(\{\mathbf{x}_1, \mathbf{x}_2\}) - D(\mathbf{x}_1) D(\mathbf{x}_2). \tag{7}$$

Using this Gaussian approximation for the density function $Q(\mathbf{y})$ we have the following approximation for the integral $\mathbf{I}$

$$\mathbf{I} \approx \mathbf{I}_1 = \int \mathcal{N}_{\Sigma_0}(\mathbf{y}_0 - \mathbf{y}) \mathcal{N}_{\Sigma_Q}(\boldsymbol{\mu}_Q - \mathbf{y}) d\mathbf{y} \tag{8}$$

$$\mathbf{I}_1 = \mathcal{N}_{\Sigma_0 + \Sigma_Q}(\mathbf{y}_0 - \boldsymbol{\mu}_Q). \tag{9}$$

A. Simulation setup

In this section we do numerical simulations to test the validity of the approximation $\mathbf{I} \approx \mathbf{I}_1$ where $\mathbf{I}$ and $\mathbf{I}_1$ are given in expressions (3) and (9). To numerically evaluate the integral $\mathbf{I}$ we first generate samples from the random finite set Ξ and use them to generate samples of the random vector $\mathbf{y}$ using the relation in (1). We use N_s sample points of the random finite set Ξ to evaluate the integral $\mathbf{I}$.

To approximate the integral $\mathbf{I}_1$ we numerically compute $\boldsymbol{\mu}_Q$ and Σ_Q from (4) and (6) by using particle approximations for $D(\mathbf{x})$ and $\tilde{D}(\{\mathbf{x}_1, \mathbf{x}_2\})$. N_v sample points are used to evaluate the integral $\mathbf{I}_1$. Note that typically we need N_s to be much larger than N_v since to efficiently sample a random finite set we need much higher number of samples than to sample from the single target state space.

We consider a two dimensional state space $\mathbf{x} = [x; y]$ consisting of the x and y coordinates of the target. For numerical analysis we consider the following linear measurement model

$$g(\mathbf{x}) = H\mathbf{x} \tag{10}$$

$$H = \begin{bmatrix} 0.1 & 0.7 \\ 0.5 & 0.5 \\ 0.8 & 0.2 \end{bmatrix} \tag{11}$$

We consider three types of random finite sets in our numerical analysis. The IIDC random finite set, the multi-Bernoulli random finite set, and the union of IIDC and multi-Bernoulli random finite set.

B. IIDC RFS

First consider Ξ to be an IIDC random finite set. Let the IIDC random finite set be described by the following normalized PHD function

$$s(\mathbf{x}) = \frac{1}{n_0} \sum_{i=1}^{n_0} \mathcal{N}_{\Sigma_i}(\mathbf{x} - \mu_i). \tag{12}$$

and let the cardinality distribution $\pi(n)$ be Poisson with mean n_0. For numerical simulation purpose we truncate the Poisson at $n = 15$ and normalize the cardinality distribution so it sums to 1. The above IIDC example models the case when n_0 targets are present with each target represented by a component in the Gaussian mixture. A sample of the IIDC random finite set is obtained by first sampling the cardinality n and then sampling n elements from the density function $s(\mathbf{x})$. We generate N_s samples from the IIDC random finite set Ξ and use it to calculate samples of the random vector $\mathbf{y}$ using the relation in (1).

The covariance matrix for each of the components is same and is set to $\Sigma_i = \text{diag}(1,1), i = 1,2,\ldots,n_0$. Also set $\Sigma_0 = 0.25\text{diag}(1,1,1)$ and $\mathbf{y}_0 = H\sum_{i=1}^{n_0} g(\mu_i)$. We vary n_0 in the range $\{3,4,5,6,7,8\}$. For each value of n_0 we run 25 different trials with the mean of the different Gaussian components μ_i in the normalized PHD function $s(\mathbf{x})$ randomly distributed over the $20m \times 20m$ region in each trial. For each trial the numerical integrals of $\mathbf{I}$ and $\mathbf{I}_1$ are evaluated 25 times and averaged to obtain their estimates $\hat{\mathbf{I}}$ and $\hat{\mathbf{I}}_1$. For evaluation of the integrals we use $N_s = 500,000$ samples points and $N_v = 10,000$ sample points. The percentage error for each trial is calculated as follows

$$\text{Percentage error} = \frac{|\hat{\mathbf{I}} - \hat{\mathbf{I}}_1|}{\hat{\mathbf{I}}} \times 100. \tag{13}$$

To understand the error introduced due to the approximation $Q(\mathbf{y}) \approx \mathcal{N}_{\Sigma_Q}(\boldsymbol{\mu}_Q - \mathbf{y})$ we pictorially compare the normalized histograms of the elements of the random vector $\mathbf{y}$ with their Gaussian density function approximations. The histograms and the approximated Gaussian density functions are shown in Figure 1. Histograms of each component of the vector $\mathbf{y}$ are shown for three different cases, $n_0 = 4, 6, \&8$. The histograms are plotted by dividing the data into 1000 uniform bins. $N_s = 500,000$ samples are used to generate the histograms. A Gaussian function is overlaid on each histogram which has mean and variance as computed from the Campbell equations. The mean and variance are calculated using $N_v = 10,000$ sample points. The average percentage error (computed over 25 trials) is shown in Table I as the number of targets n_0 is increased.

TABLE I
AVERAGE PERCENTAGE ERROR FOR IIDC RFS

n_0	percentage error
3	66.83
4	47.63
5	27.52
6	10.72
7	4.90
8	5.29

C. Multi-Bernoulli RFS

Now consider Ξ to be a multi-Bernoulli random finite set. Let there be n_0 Bernoulli components with parameters

$$\{r_i, p_i(\mathbf{x})\}, i = 1,2,\ldots n_0 \tag{14}$$

$$p_i(\mathbf{x}) = \mathcal{N}_{\Sigma_i}(\mathbf{x} - \mu_i) \tag{15}$$

The above multi-Bernoulli random finite set example represents the case when n_0 targets are present, with probability of existence r_i and each with a Gaussian density distribution. In our simulations we set $r_i \in [0.2, 1] \forall i$. Samples of the multi-

Bernoulli random finite set are generated by sampling existence variable for each component and then sampling from the corresponding density function if the component exists. The mean μ_i and covariance Σ_i are same as those considered for the IIDC case.

The histograms of elements of the vector $\mathbf{y}$ are shown in Figure 2. The individual Bernoulli components have a Gaussian density function and there are 4,6 and 8 components respectively in the three sub-figures. A Gaussian function is overlaid on each histogram which has mean and variance as computed from the Campbell equations. The average percentage error (computed over 25 trials) is shown in Table II as the number of targets n_0 is increased.

TABLE II
AVERAGE PERCENTAGE ERROR FOR MULTI-BERNOULLI RFS

n_0	percentage error
3	76.04
4	77.24
5	76.84
6	74.73
7	71.55
8	66.84

D. Union of multi-Bernoulli and IIDC RFS

We now consider the random finite set which is union of a multi-Bernoulli RFS and an IIDC RFS. For simulations we choose the multi-Bernoulli RFS with same parameters as above. The IIDC component has a uniform discrete cardinality distribution and its normalized PHD is uniform over the $20m \times 20m$ region under consideration. The sampling process is as described earlier.

The histograms and the approximated Gaussian density functions are shown in Figure 3. The average percentage error (computed over 25 trials) is shown in Table III as the number of targets n_0 of the multi-Bernoulli component is increased.

TABLE III
AVERAGE PERCENTAGE ERROR FOR UNION OF MULTI-BERNOULLI AND IIDC

n_0	percentage error
3	80.61
4	65.22
5	47.47
6	30.92
7	16.38
8	10.23

Fig. 1. Histogram of measurements calculated using 500,000 sample points from a IIDC random finite set.

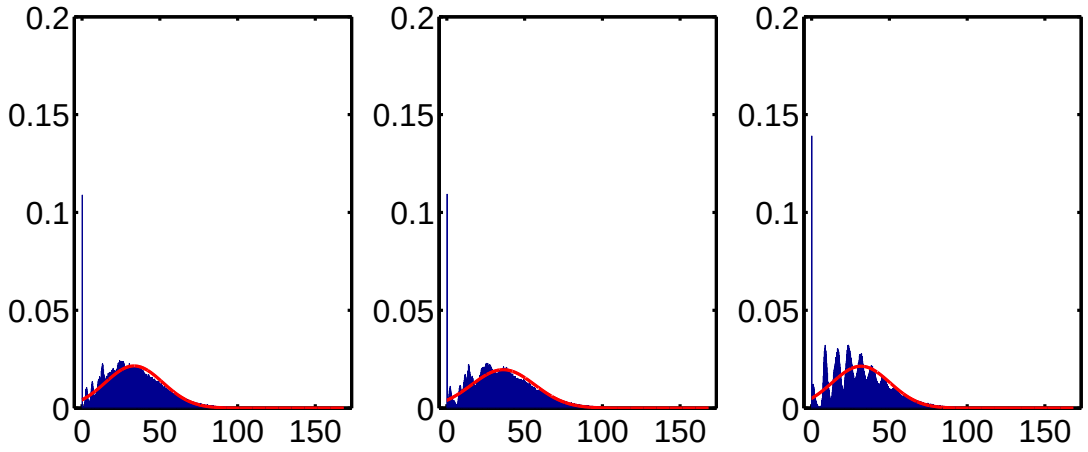

(a) (4 targets)

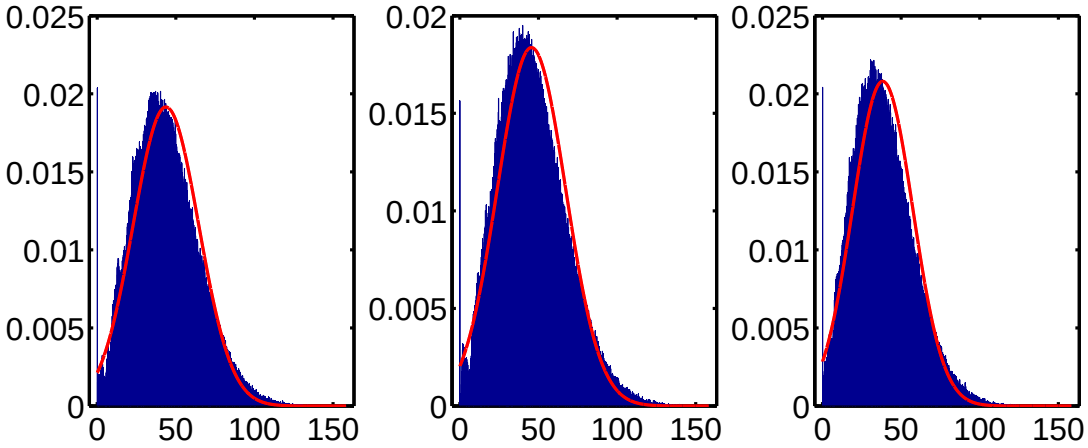

(b) (6 targets)

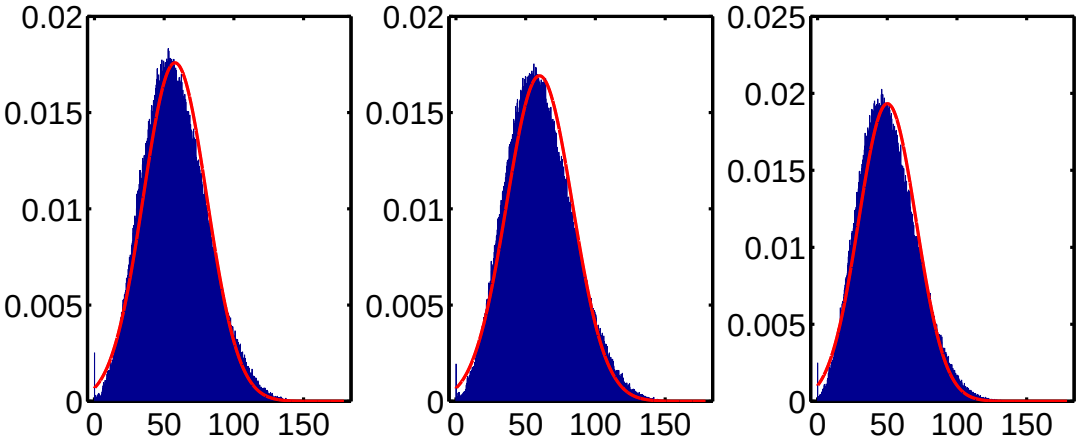

(c) (8 targets)

Fig. 2. Histogram of measurements calculated using 500,000 sample points from a multi-Bernoulli random finite set.

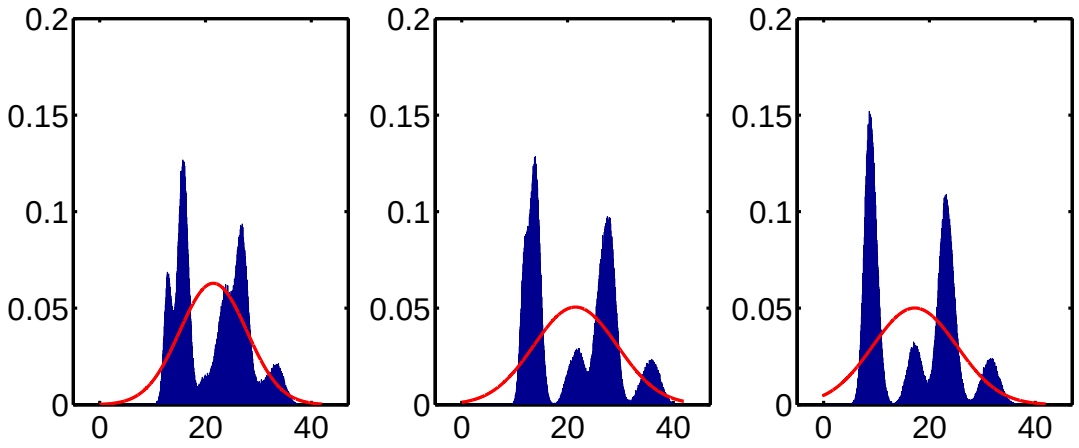

(a) (4 Bernoulli components)

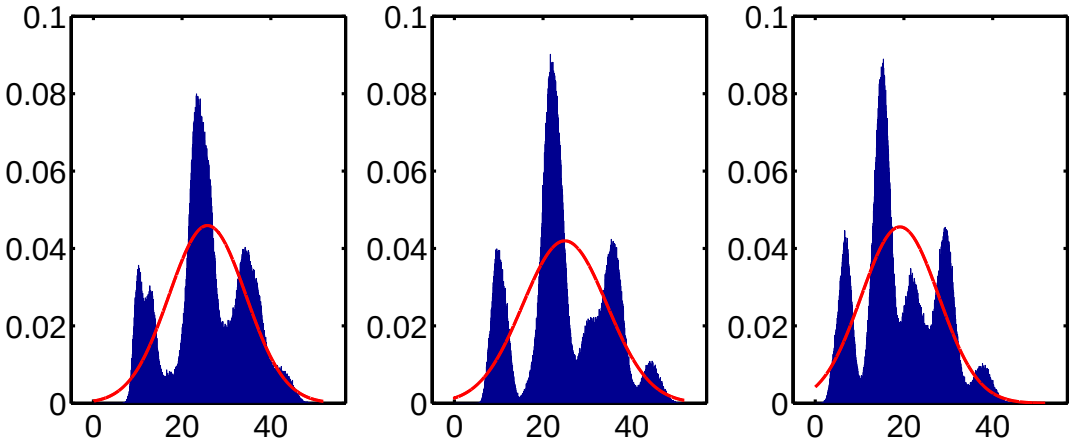

(b) (6 Bernoulli components)

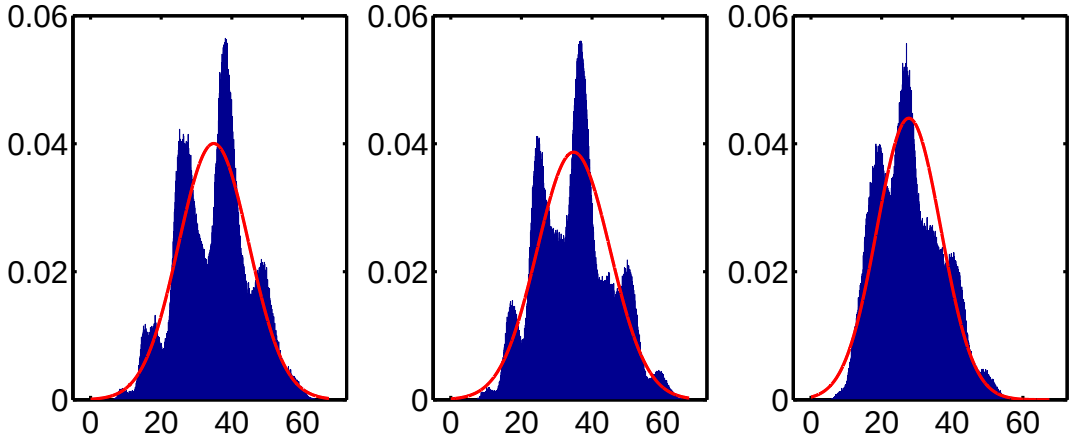

(c) (8 Bernoulli components)

Fig. 3. Histogram of measurements calculated using 500,000 sample points from union of a multi-Bernoulli and an IIDC random finite set.

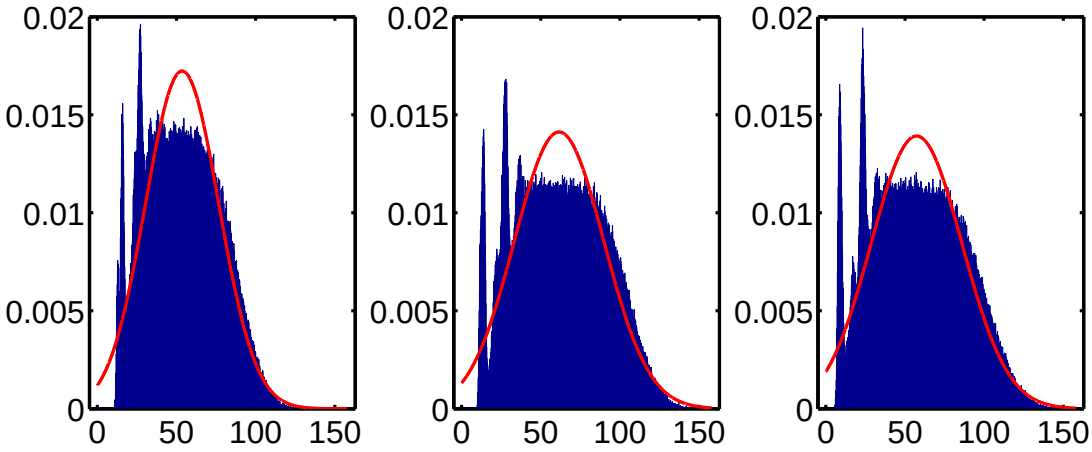

(a) (4 Bernoulli components)

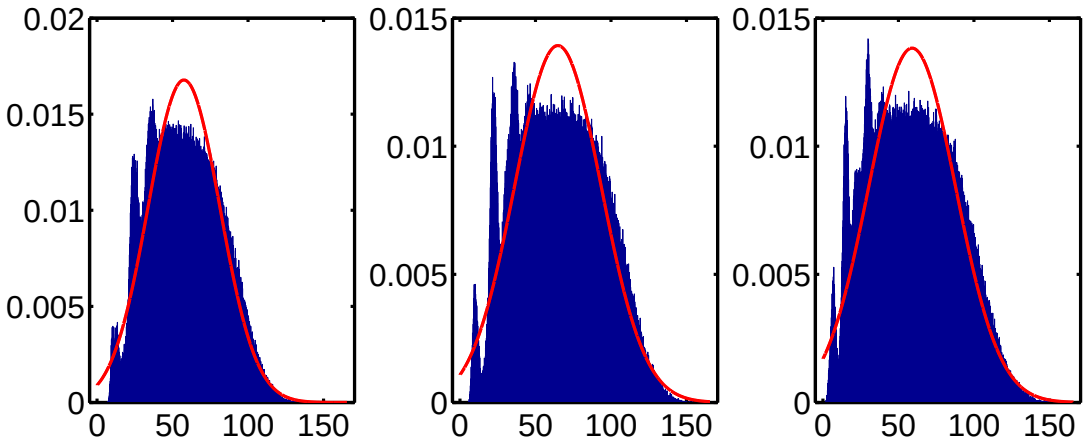

(b) (6 Bernoulli components)

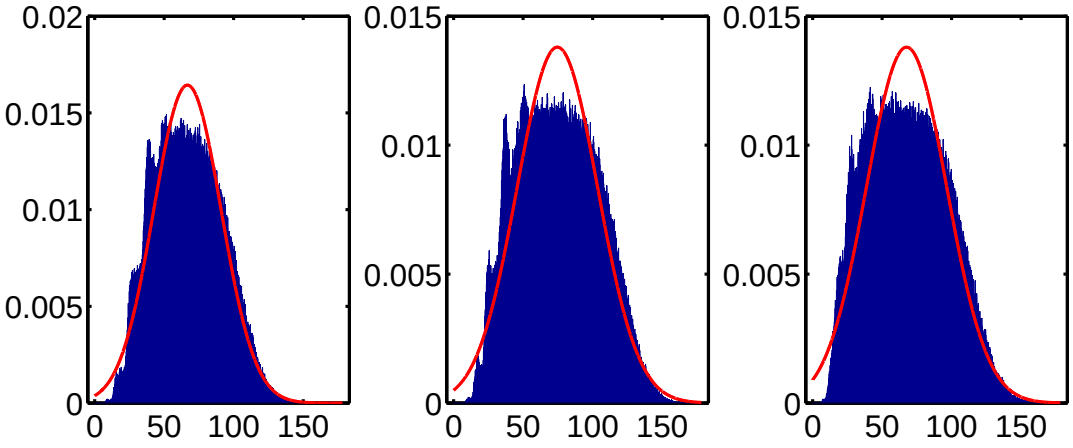

(c) (8 Bernoulli components)

E. Computation of ratio of integrals

Let the random finite set Ξ be union of independent random finite sets Ξ_A and Ξ_B with PHDs $D^A(\mathbf{x})$ and $D^B(\mathbf{x})$ and densities $f_{\Xi_A}(W)$ and $f_{\Xi_B}(W)$ respectively. All of the approximate PHD update equations for superpositional sensors [1], [2] involve computation of the ratio of integrals as follows

$$\mathbf{R}(\mathbf{x}) = \frac{\int \mathcal{N}_{\Sigma_0}(\mathbf{y}_0 - g(\mathbf{x}) - \zeta(W))\, f_{\Xi}^{A^*_{\mathbf{x}}}(W)\delta W}{\int \mathcal{N}_{\Sigma_0}(\mathbf{y}_0 - \zeta(W))\, f_{\Xi}(W)\delta W}, \tag{16}$$

where

$$f_{\Xi}^{A^*_{\mathbf{x}}}(W) = \sum_{Y \subseteq W} \frac{f_{\Xi_A}(\{\mathbf{x}\} \cup Y)}{D^A(\mathbf{x})}\, f_{\Xi_B}(W - Y) \tag{17}$$

Using change of variables the ratio $\mathbf{R}(\mathbf{x})$ can be expressed as

$$\mathbf{R}(\mathbf{x}) = \frac{\int \mathcal{N}_{\Sigma_0}(\mathbf{y}_0 - g(\mathbf{x}) - \mathbf{y}^*)\, Q^{A^*_{\mathbf{x}}}(\mathbf{y}^*) d\mathbf{y}^*}{\int \mathcal{N}_{\Sigma_0}(\mathbf{y}_0 - \mathbf{y})\, Q(\mathbf{y}) d\mathbf{y}} \tag{18}$$

Arguing as before, to make the above ratio tractable we approximate the densities $Q(\mathbf{y})$ and $Q^{A^*_{\mathbf{x}}}(\mathbf{y}^*)$ to be Gaussian and compute their mean and covariance matrix parameters using Campbell's theorem. Thus we have the approximation

$$\mathbf{R}(\mathbf{x}) \approx \mathbf{R}_1(\mathbf{x}) = \frac{\int \mathcal{N}_{\Sigma_0}(\mathbf{y}_0 - g(\mathbf{x}) - \mathbf{y}^*)\, \mathcal{N}_{\Sigma_Q^{A^*_{\mathbf{x}}}}(\boldsymbol{\mu}_Q^{A^*_{\mathbf{x}}} - \mathbf{y}) d\mathbf{y}^*}{\int \mathcal{N}_{\Sigma_0}(\mathbf{y}_0 - \mathbf{y})\, \mathcal{N}_{\Sigma_Q}(\boldsymbol{\mu}_Q - \mathbf{y}) d\mathbf{y}} \tag{19}$$

$$\mathbf{R}_1(\mathbf{x}) = \frac{\mathcal{N}_{\Sigma_0 + \Sigma_Q^{A^*_{\mathbf{x}}}}(\mathbf{y}_0 - g(\mathbf{x}) - \boldsymbol{\mu}_Q^{A^*_{\mathbf{x}}})}{\mathcal{N}_{\Sigma_0 + \Sigma_Q}(\mathbf{y}_0 - \boldsymbol{\mu}_Q)}. \tag{20}$$

To compare the error introduced in the calculation of the ratio $\mathbf{R}(\mathbf{x})$ due the Gaussian approximation we numerically evaluate $\mathbf{R}(\mathbf{x})$ and $\mathbf{R}_1(\mathbf{x})$ for different values of $\mathbf{x}$ and compute the correlation coefficient between these two ratios. We calculate these ratios for the multi-Bernoulli random finite set case when four components are present

$$\{r_i, p_i(\mathbf{x})\}, i = 1, 2, 3, 4 \tag{21}$$

$$p_i(\mathbf{x}) = \mathcal{N}_{\Sigma_i}(\mathbf{x} - \mu_i), i = 1, 2, 3, 4 \tag{22}$$

$$\Sigma_i = \text{diag}(1, 1), i = 1, 2, 3, 4. \tag{23}$$

We perform simulations for 100 different sets of randomly distributed means $\mu_i, i = 1, 2, 3, 4$ over the $20m \times 20m$ region. For each set of means the ratios $\mathbf{R}(\mathbf{x})$ and $\mathbf{R}_1(\mathbf{x})$ are numerically computed for 100 different values of $\mathbf{x}$ sampled from a Gaussian density centered around one of the means and with covariance matrix $\text{diag}(2, 2)$. Thus the correlation coefficient is computed using $10,000$ sample points.

Example 1: The probabilities of existence of the Bernoulli components are in the range $r_i \in [0.2, 1]$. The correlation coefficient is 0.22. When the probabilities of existence are increased and are in the range $r_i \in [0.5, 1]$, the correlation coefficient increases to 0.44. A bin plot of the quantities $\mathbf{R}(\mathbf{x})$ and $\mathbf{R}_1(\mathbf{x})$ is shown in Figure 4. The plot is generated by dividing the data into 10 groups. The x-axis points indicate the mean of each group. The red marker is the mean, the black marker is

the median and the blue lines indicate 10-90 percentiles. The blue diagonal line corresponds to the case $\mathbf{R}(\mathbf{x}) = \mathbf{R}_1(\mathbf{x})$. The relatively large spread of the 10-90 percentiles is captured by the low correlation coefficient of 0.44.

Example 2: We now consider the probabilities of existence of all the components to be equal $r_i = r, i = 1, 2, 3, 4$ and increase them from $r = 0.75$ to $r = 0.99$ and compute the correlation coefficient for each case. The correlation coefficients are given in Table IV. For higher values of r the correlation coefficient is high indicating the approximation is more accurate for larger values of r. A bin plot of the quantities $\mathbf{R}(\mathbf{x})$ and $\mathbf{R}_1(\mathbf{x})$ when $r = 0.95$ is shown in Figure 5. The 10-90 percentiles are narrower and the medians are closer to the diagonal line.

TABLE IV
CORRELATION COEFFICIENTS BETWEEN $\mathbf{R}(\mathbf{x})$ AND $\mathbf{R}_1(\mathbf{x})$

r	correlation coefficient
0.75	0.50
0.80	0.53
0.85	0.58
0.90	0.63
0.95	0.72
0.99	0.91

REFERENCES

[1] S. Nannuru, M. Coates, and R. Mahler, "Computationally-tractable approximate PHD and CPHD filters for superpositional sensors," *IEEE J. Sel. Topics in Sig. Proc.*, vol. 7, no. 3, pp. 410–420, Jun. 2013.

[2] S. Nannuru and M. Coates, " Multi-Bernoulli filter and hybrid multi-Bernoulli CPHD filter for superpositional sensors," *Under review*, 2015.

[3] R. Mahler, *Statistical multisource-multitarget information fusion*. Artech House, Boston, 2007.

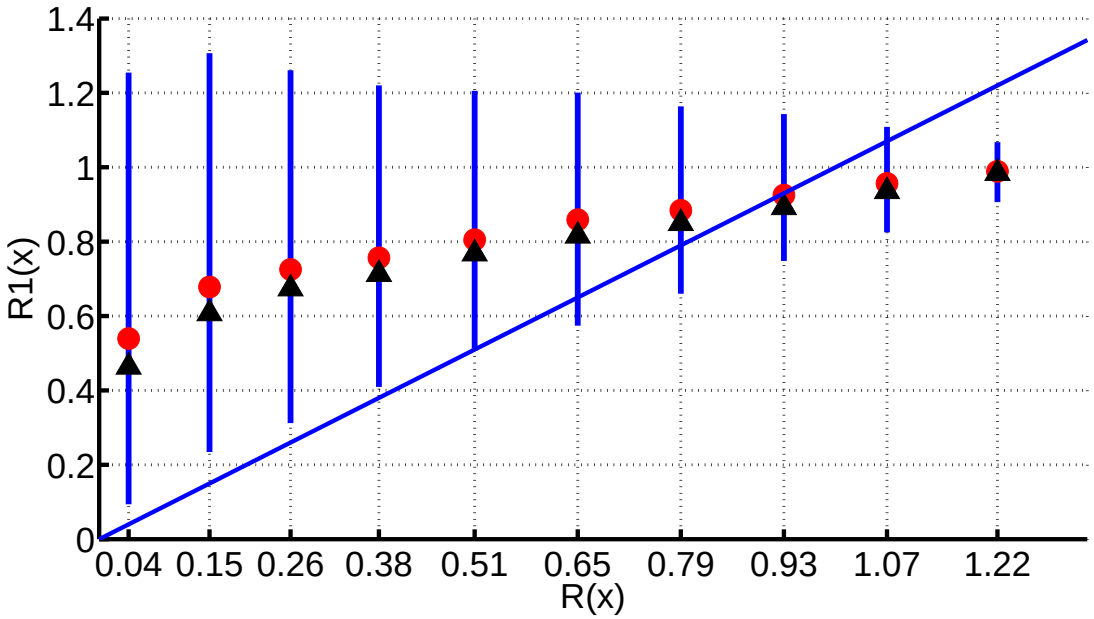

Fig. 4. Bin plot comparing the values of $\mathbf{R}(\mathbf{x})$ and $\mathbf{R}_1(\mathbf{x})$ for the case $r_i \in [0.5, 1]$. The red marker is the mean, the black marker is the median and the vertical blue lines indicate 10-90 percentiles.

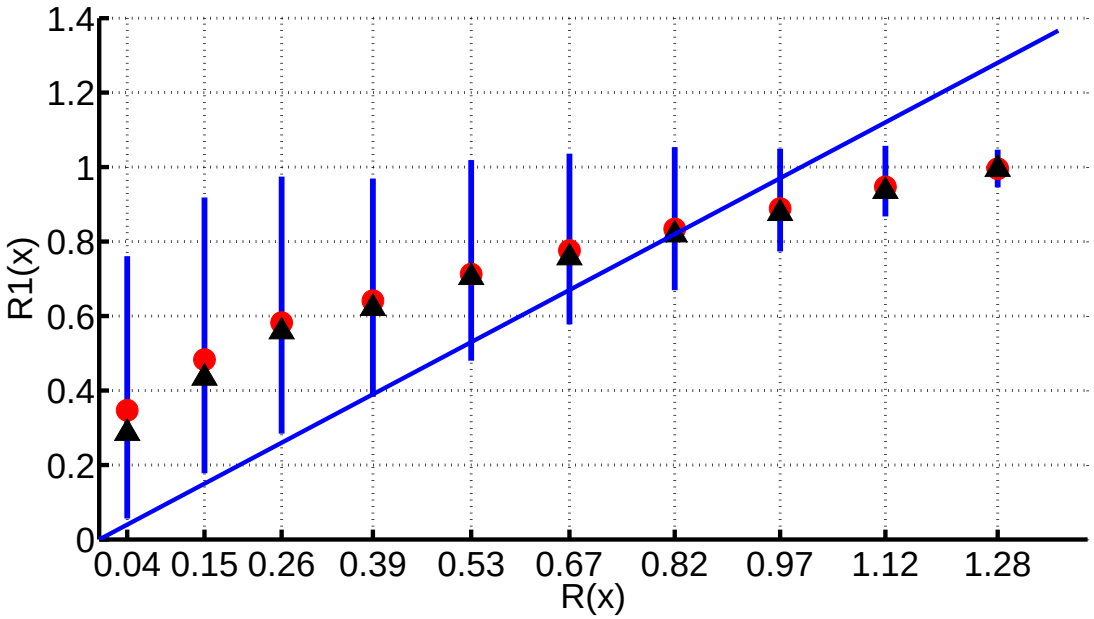

Fig. 5. Bin plot comparing the values of $\mathbf{R}(\mathbf{x})$ and $\mathbf{R}_1(\mathbf{x})$ for the case $r = 0.95$. The red marker is the mean, the black marker is the median and the vertical blue lines indicate 10-90 percentiles.